Analytical Methods

Accepted Manuscript

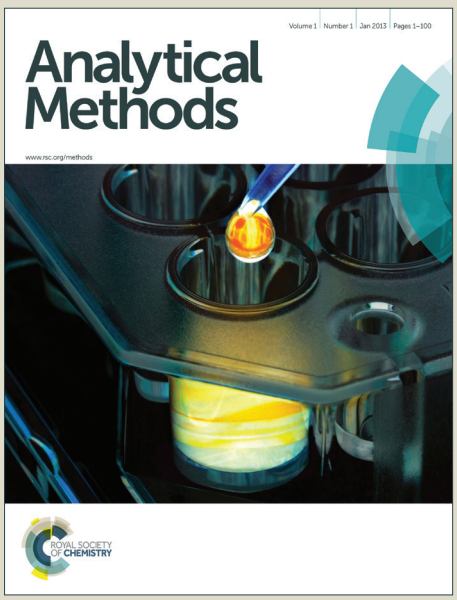

This is an *Accepted Manuscript*, which has been through the Royal Society of Chemistry peer review process and has been accepted for publication.

Accepted Manuscripts are published online shortly after acceptance, before technical editing, formatting and proof reading. Using this free service, authors can make their results available to the community, in citable form, before we publish the edited article. We will replace this *Accepted Manuscript* with the edited and formatted *Advance Article* as soon as it is available.

You can find more information about *Accepted Manuscripts* in the Information for Authors.

ROYAL SOCIETY OF CHEMISTRY

www.rsc.org/methods

Cite this: DOI: 10.1039/c0xx00000x

www.rsc.org/xxxxxx

ARTICLE TYPE

A new colorimetric protocol for selective detection of phosphate based on the inhibition of peroxidase-like activity of magnetite nanoparticles

Chuanxia Chen, [a,b] Lixia Lu, [a,b] Yu Zheng, [a,b] Dan Zhao, [a,b] Fan Yang [a] and Xiurong Yang [*a]

Received (in XXX, XXX) Xth XXXXXXXXX 20XX, Accepted Xth XXXXXXXXX 20XX

DOI: 10.1039/b000000x

A simple colorimetric assay for phosphate ion (Pi) has been established based on analyte-induced inhibition of the magnetite nanoparticles (MNPs)-catalyzed oxidation of 3, 3', 5, 5'- tetramethylbenzidine (TMB) in the presence of H_2O_2. The Fe_3O_4 MNPs can catalyze the H_2O_2-mediated oxidation of TMB and yields blue oxidized product which exhibits a maximum absorption at 652 nm. Pi could be absorbed on the surface of the Fe_3O_4 MNPs through coordinating with Fe^{3+}, inducing a reduced colorimetric signal. The colorimetric signal change (ΔA_{652}) in this process was proportional to the concentration of Pi, ranging from 0.2 μM to 200 μM. The limit of detection (S/N = 3) was as low as 0.11 μM. The as proposed Fe_3O_4 MNPs-TMB -H_2O_2 probe exhibited a high selectivity toward Pi over other relevant ions that commonly exist in water, and has been applied to Pi detection in drinking water, ground water and lake water samples with satisfactory results.

1. Introduction

Anions are ubiquitous species and play numerous indispensable roles in chemical and biological processes, as well as in environmental pollution,[1] thus plenty of efforts have been devoted for their simple, rapid and sensitive sensing and detection.[2-6] Phosphate (Pi), as an essential component of the nutritional chain of aquatic microorganisms, is a convenient indicator or tracer of pollution in bodies of water.[7-10] Phosphate is a well-known contaminant of ground water and stream water. A maximum permissible concentration of phosphate is 0.32 μM for river water and 14.3 to 143 μM for wastewater.[11] The presence of phosphate in drinking water is a health hazard. Furthermore, phosphate concentration in body fluids is an important indicator in the diagnosis of hyperparathyroidism, Vitamin D deficiency, and fanconi syndrome.[12] Consequently, Pi detection is of great significance for controlling eutrophication, monitoring drinking water quality and clinical diagnosis. Up to now, several strategies have been established for the detection of phosphate ion, including electrochemical analysis,[11, 13] chromatography,[14 - 16] spectrophotometry,[17] fluorometry,[18] and enzymatic biosensors.[19,20] However, these methods are usually challenged with sophisticated instruments, tedious experimental procedures, skilled personnel, or high expense. Thus, it is quite necessary to further develop simple, cost-effective and reliable methods for rapid and sensitive determination of Pi in both environmental and biological systems.

Spectrographic technique is simple and can be read out by the naked eye without the aid of sophisticated instruments, thus realizing the visual on-site analysis.[21] Meanwhile, colorimetry by nanomaterials has been exploited for simple and cost-effective sensing of anions owing to their unique chemical, electrical, optical and catalytic properties. Colorimetric methods utilizing nanomaterials for Pi detection have attracted significant attention. For example, Y. Kubo et al. attached isothiouronium groups onto AuNP surface and demonstrated the sensing of oxanions (AcO^-, HPO_4^{2-}, and malonate) in aqueous MeOH solution.[22] W.Q. Liu et al. have employed MA-AuNPs as a colorimetric sensing platform for phosphate based on the competition reaction between Pi and carboxylate group-modified AuNPs for Eu^{3+} ions.[23] Nevertheless, those strategies are still not well developed. The use of water-insoluble isothiouronium and the laborious premodification of the AuNPs with sulfhdryl compounds limited their application. To design a novel probe for Pi detection, new types of nanomaterials have been exploited[24, 25] and new elements except optical properties of nanomaterials such as catalytic activity may have potential applications in anion detection.

Recently, a landmark work by Yan et al. reported that Fe_3O_4 magnetic nanoparticles, usually thought to be biologically and chemically inert, possess an intrinsic enzyme mimic activity similar to that found in natural peroxidases.[26] In comparison with Horseradish Peroxidase (HRP),[27] Fe_3O_4 MNPs is low-cost, easy to obtain, more robust, and easy to be separated from the product for recycling.[28] These advantages indicate that Fe_3O_4 MNPs can be powerful tools for potential applications in medicine, biotechnology and environmental chemistry. By employing MNPs as peroxidase mimetics, several novel strategies have been developed for the detection of various chemical and biological entities, such as glucose,[29, 30] H_2O_2,[29] choline,[31] catecholamines,[32] melamine,[33] nucleic acid,[34, 35] cells[36] and proteins.[37, 38] However, up to now, there is no report on any MNPs that is used for designing the colorimetric sensing platform for inorganic anions.

Herein, we have developed a novel and convenient label-free colorimetric method for Pi detection which employed the

peroxidase-mimicking activity of MNPs. Fe_3O_4 MNPs can catalyze the H_2O_2-medicated oxidation of colorless 3, 3', 5, 5'-tetramethylbenzidine (TMB) into blue product (oxTMB), which exhibits a maximum absorption at 652 nm (A_{652}). However, the catalytic activity of Fe_3O_4 MNPs can be inhibited by Pi due to the coordination effect between Pi and Fe^{3+} on the surface of Fe_3O_4 MNPs. The colorimetric signal change in this process can be used for detection of the concentration of Pi. Based on this principle, we have achieved the detection of Pi in different samples with high selectivity and sensitivity. Thus, it is believable that the proposed sensing strategy for Pi will show great prospect in environmental monitoring, clinical diagnostic and scientific research.

2. Experimental

2.1. Reagents and apparatus

Ferric chloride was purchased from Sangon Biotech (Shanghai) Co. (China). TMB was purchased from Sigma-Aldrich (USA). Analytical grade ferrous sulfate, H_2O_2, sodium salts of anion (PO_4^{3-}, $H_2PO_2^-$, S^{2-}, SO_4^{2-}, SO_3^{2-}, F^-, Cl^-, Br^-, BrO_3^-, SCN^-, NO_3^-, $C_2O_4^{2-}$), chloride salts of ion (Na^+, K^+, Al^{3+}, Ba^{2+}, Cu^{2+}, Co^{2+}, Cr^{3+}, Ni^{2+}, Zn^{2+}), $Ca(NO_3)_2$, $MgSO_4$, PbC_2O_4 were obtained from Beijing Chemical Reagent Co. (China). All reagents were used as received. Acetate buffer solutions with different pH values were prepared by varying the ratio of 0.2 M acetate acid to 0.2 M sodium acetate and diluted to the concentration demanded. The water used throughout the experiment was purified by a Milli-Q water system (resistivity 18.25 MΩ cm, Millipore, ultrapure water).

UV-vis absorption spectra were recorded with a Cary 50 UV-vis spectrophotometer (Varian). High-resolution transmission electronic microscopy (HRTEM) images were obtained on a Tecnai G2 F20 (FEI) transmission electron microscope operated at 200 kV. The sample for TEM characterization was prepared by evaporating a droplet of dilute solution onto double networking carbon-coated coppergrids. Photos were taken with a commercially digital camera. The X-ray photoelectron spectroscopy (XPS) samples on highly cleaned silicon wafers were analyzed by an ESCALAB MK II spectrometer (VG Scientific) with Al Kα radiation as the X-ray source. Peak positions were internally referenced to the C1s peak at 284.6 eV. X-ray powder diffraction (XRD) study was carried out using Bruker D8 Advance (Bruker AXS, Germany) with a graphite monochromator using Cu Kα radiation.

2.2. Synthesis of Fe_3O_4 MNPs

Fe_3O_4 MNPs were synthesized according to Massart's method.[39] Under vigorous stirring, 5 mL freshly prepared aqueous mixture of ferric chloride (4 mL, 1 M in 2 M HCl) and ferrous sulfate (1 mL, 2 M in 2 M HCl) was added to ammonia solution (50 mL, 0.7 M) quickly. The mixture was stirred continuously for another 30 min at room temperature, then, the formed black precipitate was collected on the vessel wall by an external permanent magnet, rinsed with ultrapure water four times. The obtained product was then re-dispersed in ultrapure water water and subjected to ultrasound for 30 min to make the final concentration to be ~ 4.4 mg/mL (refereed as Fe_3O_4 MNPs stock solution).

2.3. Detection of phosphate anions using Fe_3O_4 MNPs

5 μL of 1.1 mg/mL Fe_3O_4 MNPs colloidal solution, 20 μL of phosphate solutions with different concentrations were added into 147 μL of 0.2 M acetate buffer (pH 4.0) respectively. The mixture was vortexed thoroughly and incubated at ambient temperature for 5 min. Subsequently, 20 μL of 5 mM TMB and 8 μL of 20 mM H_2O_2 were added into the solution. The mixture was vortex-mixed and incubated in a water bath at 50 °C for 20 min. The final solution was used for absorbance measurement.

2.4. Analysis of real samples

The drinking water and ground water samples were used without further treatment, lake water sample was filtered through 0.22 μm membrane, and all the samples were detected according to the following procedure with three replicates: 5 μL of 1.1 mg/mL Fe_3O_4 MNPs colloidal solution and 20 μL real samples were added into 147 μL of 0.2 M acetate buffer (pH 4.0), then the mixture was vortexed thoroughly and incubated at ambient temperature for 5 min. Subsequently, 20 μL of 5 mM TMB and 8 μL of 20 mM H_2O_2 were added into the solution. The mixture was vortex-mixed and incubated at 50 °C water bath for 20 min. The final solution was used for absorbance measurement.

3. Results and discussion

3.1. Mechanism of the Pi detection

The formation of Fe_3O_4 MNPs was confirmed by HRTEM, XPS and XRD characterization. HRTEM images of Fe_3O_4 MNPs (Fig.S1 A, Supporting Information) show that the diameter of the prepared Fe_3O_4 MNPs distributed in the range of 6~10 nm, roughly spherical in shape. The binding energies of Fe $2p_{3/2}$ and Fe $2p_{1/2}$ for the Fe_3O_4 MNPs sample were 710.6 and 724.1 eV; simultaneously, $2p_{3/2}$ for Fe_3O_4 did not have a satellite peak (Fig.S1 C，Supporting Information). The XRD pattern shows signals at 2θ=30°, 35°, 37°, 42°, 56.8, 62.5° (220, 311, 222, 400, 511, 440) (Fig.S1 D，Supporting Information). These diffraction peaks could be characterized as face-centered cubic phase of Fe_3O_4, which are consistent with the value reported in the literature (JCPDS file No. 19–629). The HRTEM, XPS and XRD spectra revealed the formation of Fe_3O_4 MNPs. The aqueous solution of the MNPs was black in color and had no remarkable absorption peak in the wavelength range of 400-800 nm. Although no appreciable change in size or disperse state was observed using HRTEM (Fig.S1 A, B，Supporting Information),

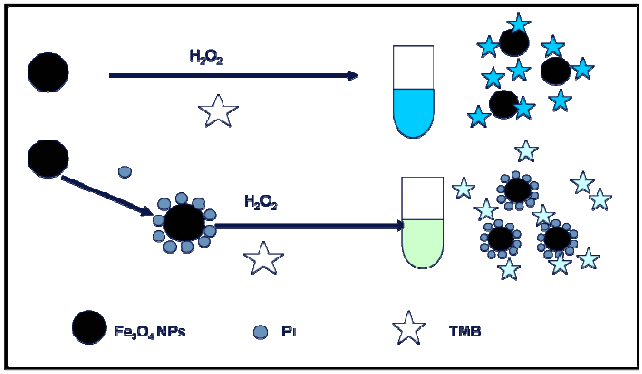

Scheme1 Pi detection based on the Fe_3O_4 MNPs-TMB-H_2O_2 system.

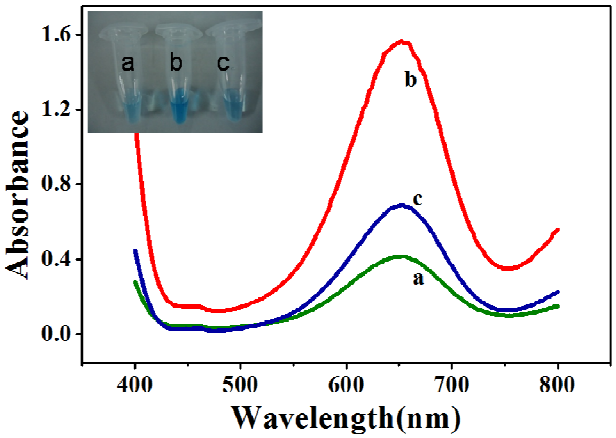

Fig.1 UV–vis absorption spectra for reaction solutions of TMB-H_2O_2 (a), Fe_3O_4 MNPs-TMB-H_2O_2 (b) and Fe_3O_4 MNPs-TMB-H_2O_2-Pi (c). MNPs: 27.5 μg/mL, TMB: 2.5 mM, H_2O_2:4.0 mM, Pi: 100 μM, HAc-NaAc buffer solution (0.2 M, pH 4.0). The insets are the photographs showing respective colorimetric responses.

Pi had some enhancement effect on the absorption curve of Fe_3O_4 MNPs (Fig.S2, Supporting Information), which preliminary demonstrated that binding event occurred between Pi and Fe^{3+}.

Pi can coordinate with Fe^{3+} on the surface of MNPs effectively based on the facts that Pi has high binding constants with Fe^{3+}.[40,41] The coordination of Pi with Fe^{3+} may affect the surface properties and catalytic ability of Fe_3O_4 MNPs. Scheme 1 illustrates the basic principle of Pi detection based on the Fe_3O_4 MNPs-TMB-H_2O_2 system. In the absence of Pi, Fe_3O_4 MNPs in the solution keep their normal peroxidise-mimicking activity, which can catalyze the oxidation of TMB by H_2O_2, giving a blue oxidation product (oxTMB). However, when Pi is added, Pi will adsorb onto the surface of Fe_3O_4 MNPs through coordinating with Fe^{3+}. The complexes formed effectively keep the substrate away from the MNPs, which is required for the peroxidase-like reaction. In this manner, Pi inhibits the catalytic activity of Fe_3O_4 MNPs, thus leading to significantly reduced colorimetric signal. The decrease of the catalytic activity of Fe_3O_4 MNPs is directly dependent on the concentration of Pi. In this case, the absorption intensity of oxTMB at 652 nm decreases with increasing the concentration of Pi. Therefore, the Fe_3O_4 MNPs-TMB-H_2O_2 system can serve as a colorimetric probe for the quantitative detection of Pi.

To demonstrate these hypotheses, we monitored Fe_3O_4 MNPs-catalyzed oxidation of TMB in the absence and presence of Pi. Curve a in Fig.1 shows that mixture of 2.5 mM TMB and 4.0 mM H_2O_2 in 0.2 M NaAc-HAc buffer (pH 4.0) produced a weak absorption at 652 nm (A_{652}). The addition of 27.5 μg/mL MNPs to the above mixture produced a much stronger A_{652} (curve b in Fig.1), indicating that Fe_3O_4 MNPs unambiguously catalyze the oxidation reaction of the substrate TMB with H_2O_2. However, when 100 μM Pi was present in a solution containing MNPs, the addition of the same concentration of TMB and H_2O_2 resulted in weaker A_{652} (curve c in Fig.1). This could be attributed to the ability of Pi to coordinate on the surface of Fe_3O_4 MNPs, thereby inhibiting the catalytic activity of Fe_3O_4 MNPs. From all the above results, it can be concluded that Fe_3O_4 MNPs-TMB-H_2O_2 system is suitable for the sensitive determination of Pi.

3.2. Optimization of experimental conditions

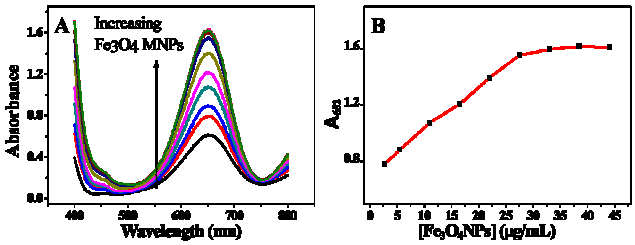

Fig.2 (A) UV–vis absorption spectra of the TMB-H_2O_2 system containing various concentrations of Fe_3O_4 MNPs. (B) The linear dependence of A_{652} on the Fe_3O_4 MNPs concentration. TMB: 2.5 mM, H_2O_2:4.0 mM, HAc-NaAc buffer solution (0.2 M, pH 4.0).

To find the optimum experimental conditions, the effects of concentration of Fe_3O_4 MNPs, the pH of the reaction buffer, the incubation temperature and the reaction time were studied in detail.

3.2.1. Effect of concentration of Fe_3O_4 MNPs

The concentration of Fe_3O_4 MNPs is a key factor for this sensing system. In order to choose a suitable concentration of MNPs, the relationship between A_{652} and the concentration of MNPs was examined. Fig.2A shows the absorption spectra of the TMB-H_2O_2 system containing various concentrations of MNPs. As shown in Fig.2B, the A_{652} value was directly proportional to the concentration of MNPs ranging from 2.75 to 27.5 μg/mL. The experimental results revealed that the higher the concentration of Fe_3O_4 MNPs, the higher the catalytic efficiency of the reaction and thus the Fe_3O_4 MNPs-TMB-H_2O_2 probe was more sensitive to Pi. Whereas when the concentration of MNPs was higher than 27.5 μg/mL, the A_{652} almost kept unchanged. Considering these effects, 27.5 μg/mL Fe_3O_4 MNPs solution was selected for the subsequent study in this sensing system.

3.2.2. Effect of pH

Another driving factor for the as-proposed sensing platform is the buffer pH value as it has effects on the ΔA_{652} ($\Delta A_{652}= A_{652}^0-A_{652}$) and the selectivity of the probe toward Pi. A_{652}^0 and A_{652} correspond to the absorbance intensity at 652 nm of the MNPs - TMB-H_2O_2 probe in the absence and presence of Pi, respectively. The isoelectric point of Fe_3O_4 MNPs is about 6.8 (Fig.S3, Supporting Information), which is in accordance with the value reported before (6.5-6.8).[42, 43] MNPs are positively charged below pH 6.8 and negatively charged as pH value exceeds 6.8.The high positive value of zeta potential might mean higher catalytic ability [44] and easily adsorption of Pi on the surface of nanoparticles. Therefore, we examined the influence of pH values that below 6.8. The relationship between the catalytic ability of the Fe_3O_4 MNPs and the buffer pH values is shown in Fig.3. The absorption intensity at 652 nm of Fe_3O_4 MNPs-TMB-H_2O_2 and Fe_3O_4 MNPs-TMB-H_2O_2-Pi systems both decreased as the pH value increased. This demonstrated that Fe_3O_4 MNPs exhibited better catalytic ability at relatively lower buffer pH values. Additionally, ΔA_{652} decreased gradually with the increasing value of pH as displayed in Fig.3. Thus, a lower pH value was preferable to get a higher ΔA_{652}. Nevertheless, S^{2-} would have a significant enhancement effect on this system when buffer pH

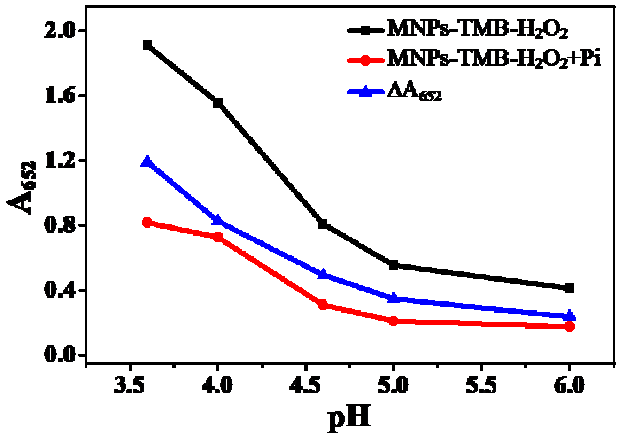

Fig.3 Plot of A_{652} of Fe_3O_4 MNPs-TMB-H_2O_2, Fe_3O_4 MNPs-TMB-H_2O_2+Pi system and ΔA_{652} versus pH (0.2 M NaAc-HAc buffer with different pH). MNPs: 27.5 μg/mL, TMB: 2.5 mM, H_2O_2:4.0 mM, Pi: 100 μM.

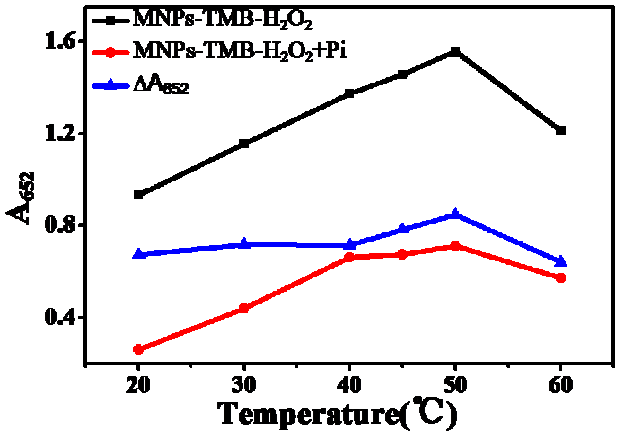

Fig.4 Plot of A_{652} of Fe_3O_4 MNPs-TMB-H_2O_2 system and Fe_3O_4-MNPs-TMB-H_2O_2+Pi system versus temperature, and ΔA_{652}versus temperature. MNPs: 27.5 μg/mL, TMB: 2.5mM, H_2O_2: 4.0 mM, Pi: 100 μM, HAc-NaAc buffer solution (0.2 M, pH 4.0).

value is too low (Fig.S4, Supporting Information), which might be attributed to the formation of the FeS/H_2S system.[45] Accordingly, to avoid this interference, pH 4.0 was chosen for the following measurement in order to achieve a better sensing signal and selectivity.

3.2.3. Effect of the temperature and reaction time

The effect of the temperature on ΔA_{652} was investigated and the results are shown in Fig.4. From Fig.4, we can see that although A_{652} values of Fe_3O_4 MNPs-TMB-H_2O_2 and Fe_3O_4 MNPs-TMB-H_2O_2-Pi systems gradually increased with the increase of temperature in the range of 20-40 °C, ΔA value changed little. When the temperature increased from 40 to 60 °C, ΔA_{652} increased first and then decreased, giving a maximum value at 50 °C. Thus, 50 °C was taken as the optimal reaction temperature.

The influence of the reaction time for catalytic oxidation of TMB was also evaluated. Pi and Fe_3O_4 MNPs were pre-incubated for 5 min to ensure a completed coordination between the Pi and Fe^{3+} (Fig.S5, Supporting Information) before the catalytic

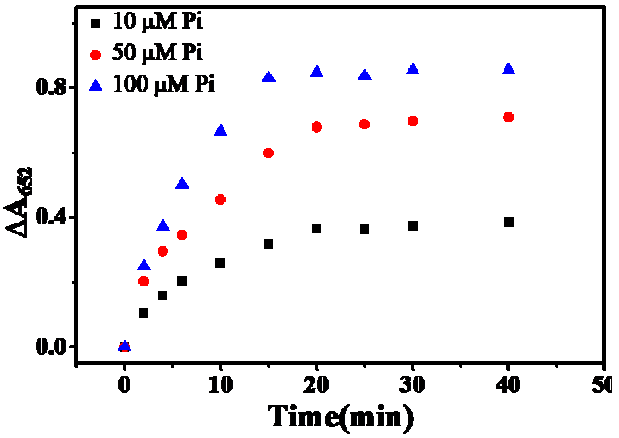

Fig.5 Plot of ΔA_{652} versus time of catalytic reaction under various concentrations of Pi at 50 °C. MNPs: 27.5 μg/mL, TMB: 2.5 mM, H_2O_2: 4.0 mM, HAc-NaAc buffer solution (0.2 M, pH 4.0).

reaction was carried out. As described in Fig. 5, ΔA_{652} gradually increased with increased catalytic reaction time, and reached the maximum when reaction time was 20 min, then leveled off. Therefore, 20 min was adopted as the optimal catalytic reaction time.

3.2.4. Interference study

To evaluate the selectivity of this sensing system towards Pi (100 μM), we measured the colorimetric response of this sensing system to some common anions, including Cl^-, Br^-, BrO_3^-, NO_3^-, SO_4^{2-}, SO_3^{2-}, SCN^-, $C_2O_4^{2-}$, $H_2PO_2^-$ (all 1.0 mM), F^- and S^{2-} (0.1 mM). The results in Fig. 6 show that only Pi could induce a drastic decrease in the colorimetric intensity, whereas no obvious colorimetric changes were observed in the presence of other ions even their concentrations were ten times greater than that of Pi, indicating that the sensing system had a good selectivity towards Pi. This excellent selectivity could be attributed to the coordination reaction between the Pi and Fe^{3+} as discussed above. Besides, some metallic ions, including Na^+, K^+, Ca^{2+}, Mg^{2+}, Al^{3+}, Ba^{2+}, Cu^{2+}, Co^{2+}, Ni^{2+}, Zn^{2+}, Pb^{2+} (all 0.1 mM), were also tested for their colorimetric responses. None of them caused significant colorimetric changes. Since the occurrence of the catalytic reaction is attributed to Fe^{3+} and Fe^{2+} ions on the surface of the Fe_3O_4 nanoparticles, Fe^{3+} and Fe^{2+} interfere greatly with the assay. Nevertheless, the interferences can be ignored when their concentrations were below 10 μM (Fig.S6 A), which was higher than the limits value of iron in surface water (~5.36 μM) according to the Environmental Quality Standards for Surface Water of the People's Republic of China. Therefore, the interference from iron ions can be neglected for most of the surface water samples. For the detection of Pi in solutions containing high levels of the two ions, pre-treatment of samples to remove them is required. Results in Fig.S6 B illustrated that the interference from ferric ion can be eliminated by a cation-exchange column. Phenol can coordinate with Fe^{3+} and thus interferes with the assay.[32] The threshold for phenol in environmental water is 0.5 mg/L (less than 5.3 uM) according to the Chinese National Standards (GB22574−2008). Nevertheless, phenol was generally not detected in tap water, well water, river water and lake water.[46-48] For this reason, the interference from phenol can be ignored. Besides the anions, some metallic ions,

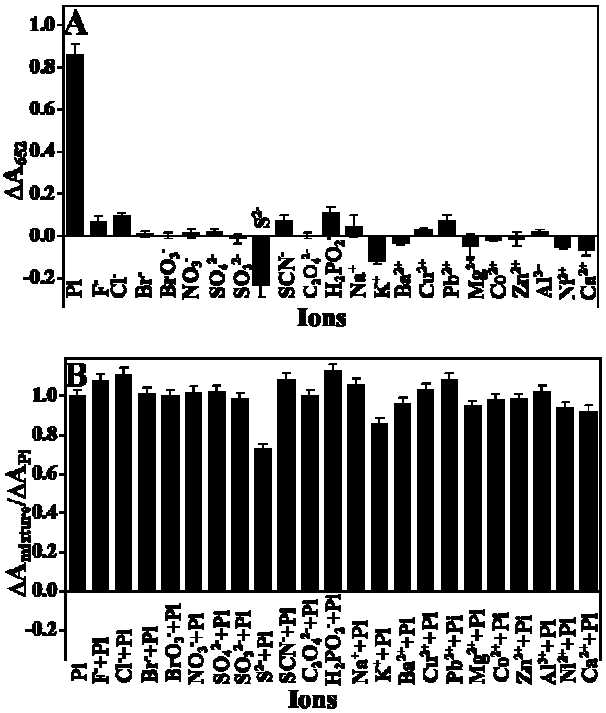

Fig.6 (A) The ΔA_{652} response of the assay system toward phosphate and other anions or metallic ions. (B) Interference study of the sensor in the presence of a mixture of Pi and another anion or metallic ion (0.1 mM of Pi, PPi, F^-, S^{2-}, and cations, 1.0 mM of other anions). MNPs: 27.5 μg/mL, TMB: 2.5 mM, H_2O_2: 4.0 mM, HAc-NaAc buffer solution (0.2 M, pH 4.0).

including Na^+, K^+, Ca^{2+}, Mg^{2+}, Al^{3+}, Ba^{2+}, Cu^{2+}, Co^{2+}, Ni^{2+}, Zn^{2+}, Pb^{2+} (all 0.1 mM), were also tested for colorimetric responses. None of them caused significant colorimetric changes.

3.3. Detection of Pi

Under the optimized conditions discussed above, the linear response range of the sensing system was measured. As shown in Fig.7A, the absorption intensity at 652 nm was highly sensitive to Pi and decreased gradually as the concentration of Pi was

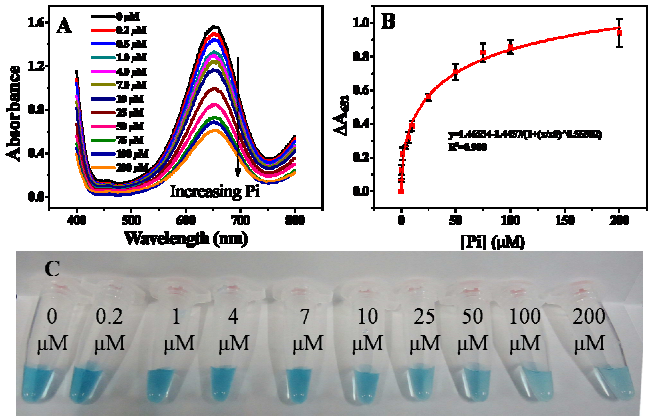

Fig.7 (A) UV–vis absorption spectra of assay systems containing different concentrations of Pi. (B) The correlation curve between the change of absorbance at 652 nm (ΔA_{652}) and the concentration of Pi. (C) Photographs of assay systems containing different concentrations of Pi. MNPs: 27.5 μg/mL, TMB: 2.5 mM, H_2O_2: 4.0 mM, HAc-NaAc buffer solution (0.2 M, pH 4.0).

increased from 0.2 to 200 μM. Accordingly, ΔA_{652} increased gradually with the concentration of Pi ranging from 0.2 to 200 μM (Fig.7B) and the calibration curve showed logistic function-shaped basically, the correlation was ΔA_{652}=1.46534-1.4457/ (1 + ([Pi]/60.807)$^{0.55502}$), R^2=0.98797. The theoretical limit of detection, LOD, was calculated to be 0.11μM, at a signal-to-noise ratio of 3. The value of the LOD was comparable to previously reported values obtained from the electrochemical analysis,[11] spectrophotometry,[17] fluorometry,[18] and enzymatic biosensors.[20] The digital photo in the inset of Fig. 7 indicates that a containment level of 4.0 μM can be easily read out by naked eyes.

3.4. Detection of Pi in practical samples

To investigate the applicability of the sensing system in real samples, we used the established sensor to determine Pi in drinking water, ground water and lake water. The three water samples were spiked with two concentration levels of Pi anions respectively, and three replicas of each level were analyzed by the proposed method. The experimental results, as shown in Table 1, demonstrated the acceptable quantitative recoveries of all samples. The percentage recoveries were among 97.8–113.6% and the RSD was less than 6.5%. Additionally, the results obtained by the present method are in accordance with those obtained by the standard molybdenum-blue method,[49] indicating the feasibility of the sensing system in practical use.

Table 1 Results of Pi determination and recoveries in water samples

Samples	The present method (μM)	Molybdenum-blue method (μM)	Added (μM)	Found (μM)	Recovery (%)	RSD (n=3, %)
A	undetectable	undetectable	5 20	4.96 19.56	99.2 97.8	1.95 0.60
B	3.60	3.74	5 20	5.68 21.8	113.6 109	5.57 6.42
C	undetectable	undetectable	5 20	5.30 20.66	106 103.3	3.90 0.71

[a] A is drinking water sample, B is ground water sample, C is lake water sample

4. Conclusions

In summary, a simple method is proposed herein for the determination of trace levels of Pi based on the shielding of Fe_3O_4 MNPs' catalytic ability. Assay samples that do not contain Pi display intense colorimetric responses while those containing Pi show significantly reduced colorimetric signals. This difference can be easily detected using UV-vis spectrophotometry and used for Pi detection. The change of the colour and the absorption at 652 nm of the Fe_3O_4 MNPs-TMB-H_2O_2 sensing system might be attributed to the coordination of Pi and Fe^{3+}. The assay has advantages of rapidity, low cost, high sensitivity and selectivity, thus proving to be a powerful tool in environment science and water quality monitoring.

Acknowledgements

This work was supported by the National Natural Science Foundation of China (No. 21175124), the National Key Basic Research Development Project of China (No. 2010CB933602)

and the Development Project of Science and Technology of Jilin Province (No. 20125090).

Notes and references

[a] *State Key Laboratory of Electroanalytical Chemistry, Changchun Institute of Applied Chemistry, Chinese Academy of Sciences, Changchun, Jilin 130022, China Fax:* +86 431 85689278*; Tel:* +86 431 85262056; E-mail: xryang@ciac.ac.cn

[b] *Graduate School of the Chinese Academy of Sciences, Beijing 100049, China.*

† Electronic Supplementary Information (ESI) available: Fig.S1-S6. See DOI: 10.1039/b000000x/

1 P.D. Beer and E.J. Hayes, *Coord. Chem. Rev.*, 2003, **240**, 167-189.
2 X.Y. Zhao, Y. Liu and K.S. Schanze, *Chem.Commun.*, 2007, **28**, 2914-2916.
3 J. Zhang, C.X. Chen, X.W. Xu, X.L. Wang and X.R.Yang, *Chem. Commun.*, 2013, **49**, 2691-2693.
4 Y.L. Liu, K.L.Ai, X.L.Cheng, L.H. Huo and L.H. Lu, *Adv. Funct. Mater.*, 2010, **20**, 1-6.
5 F. Qu, N.B. Li and H. Q. Luo, *Anal. Chem.*, 2012, **84**, 10373-10379.
6 T.Y. Zhou, M.C. Rong, Z.M. Cai, C.Y. Yang and X. Chen，*Nanoscale*, 2012, **4**, 4103-4106.
7 J.H. Ryther and W.M. Dunstan, *Science*, 1971, **171**, 1008-1013.
8 B.Y. Spivakov, T.A. Maryutina and H. Muntau, *Pure Appl. Chem.*, 1999, **71**, 2161-2176.
9 C.P. Mainstone and W. Parr, *The Science of the Total Environment*, 2002, **282-283**, 25-47.
10 P.J.A. Withers and H.P. Jarvie, *science of the total environment*, 2008, **400**, 379-395.
11 W.-L. Cheng, J.-W. Sue, W.-C. Chen, J.-L. Chang and J.-M. Zen, *Anal. Chem.*, 2010, **82**, 1157-161.
12 H. Kawasaki, K. Sato, J. Ogawa, Y. Hasegawa and H.Yuki, Anal. Biochem., 1989, 182, 366-370.
13 S. Cosnier, C. Gondran, J.-C. Watelet, W.D. Giovani, R.P. M. Furriel and F.A. Leone, *Anal. Chem.*,1998, **70**, 3952-3956.
14 J.B. Quintana, R. Rodil and T. Reemtsma, *Anal. Chem.*, 2006, **78**, 1644-1650.
15 M. Colina and P. H. E. Gardiner, *J. Chromatogr.*, 1999, **A 847**, 285-290.
16 H.M. Qiu, J.J. Geng, C. Han and H.Q. Ren, *Chinese J. Anal. Chem.* , 2013, **12**, 1910-1914.
17 C.M. Li, Y.F. Li, J. Wang and C.Z. Huang, *Talanta*, 2010, **21**, 1339-1345.
18 A.K. Dwivedi, G. Saikia and P.K. Iyer, *J. Mater. Chem.*, 2011, **21**, 2502-2507.
19 W.C. Mak, C.Y. Chan, J. Barford and R. Renneberg, *Biosens. Bioelectron.*, 2003, **19**, 233-237.
20 M.A. Rahmana, D.-S. Park, S.-C. Chang, C.J. McNeil and Y.-B. Shim, *Biosens. Bioelectron.*,2006, **21**, 1116-1124.
21 B. Kong, A.W. Zhu, Y.P. Luo, Y. Tian, Y.Y. Yu and G.Y. Shi, *Angewandte Chemie International Edition*, 2011, **50**, 1837-1840.
22 Y. Kubo, S. Uchida and Y. Kemmochi, T. Okubo, *Tetrahedron Letters*,2005, **4** , 4369-4372.
23 W.Q. Liu, Z.F. Du, Y. Qian and F. Li, *Sensors and Actuators B*, 2103, **176**, 927-931.
24 H.X. Zhao, L.Q. Liu, Z D. Liu, Y. Wang, X.J. Zhao and C.Z. Huang, *Chem. Commun.*, 2011, **47**, 2604-2606.
25 J.-M. Bai, L. Zhang, R.-P. Liang and J.-D. Qiu, *Chem. Eur. J.*, 2013, **19** ,) 3822-3826
26 L. Gao, J. Zhuang, L. Nie, J. B. Zhang and Y .N. Zhang, Nanotechnol., 2007, **2** , 577-583.
27 X.J. Chen, Y.Z. Wang, Y.Y. Zhang, Z.H. Chen, Y. Liu, Z.L. Li and J.H. Li, Anal. Chem. 2014,86,4278-4286.
28 Y.Z. Wang, K.Qu, L.H.Tang , Z.L.Li, E. Moore, X.Q. Zeng, Y. Liu, J.H. Li, Trends Anal. Chem., 2014, 58, 54-70.
29 H. Wei and E.K. Wang, *Anal. Chem.*,2008, **80**, 2250-2254.
30 C.-J. Yu, C.-Y. Lin, C.-H. Liu, T.-L. Cheng, W.-L. Tseng, *Biosens. & Bioelectron.*, 2010, **26**, 913-917.
31 C.-H. Liu, W.-L. Tseng, *Anal. Chim. Acta*, 2011, **703**, 87-93.
32 C.-H. Liu, C.-J. Yu and W.-L. Tseng, *Analytica Chimica Acta*, 2012, **745**, 143-148.
33 N. Ding, N.Yan, C.L. Ren and X.G. Chen, *Anal.Chem.*, 2010, **82**, 5897-5899.
34 K.S. Park, M.I. Kim, D.-Y. Cho and H.G. Park, *small*, 2011, **7**, 1521-1525.
35 R. Thiramanas, K. Jangpatarapongsa, P. Tangboriboonrat and D. Polpanich, *Anal. Chem.*, 2013, **85**, 5996-6002.
36 C. Kaittanis, S. Santra and J. M. Perez, *J. Am. Chem. Soc.*, 2009, **131**, 12780-12791.
37 L.Z. Gao , J.M. Wu , S. Lyle , K. Zehr , L.L. Cao and D. Gao , *J. Phys. Chem. C*, 2008, **112**, 17357-7361.
38 X.N. Li, F. Wen, B. Creran, Y. Jeong, X.R. Zhang, V.M. Rotello, Small, 2012, **8**, 3589-3592.
39 R. Massart, *IEEE Trans. Magn.*, 1981, **17**, 1247-1248.
40 C.W. Childs, *J. Phys. Chem.*, 1969, **73**, 2956-2960.
41 P.-H. Li, J.Y. Lin, C.T. Chen, W.R. Ciou, P.-H. Chan, L.Y. Luo, H.-Y. Hsu, E. W.-G. Diau and Y.-C.Chen, *Anal. Chem.*, 2012, **84**, 5484-5488.
42 G.A. Park., *Chem. Rev.*, 1965,177-198.
43 Z.G. Peng, K. Hidajat and M.S. Uddin, J. Colloid Interface Sci., 2004, **271**, 277-283.
44 Y. Jv, B.X. Li and R. Cao, *Chem. Commun.*, 2010, **46**, 8017–8019.
45 M. Dörr, T. Alpermann and W. Weigand, *Orig Life Evol Biosph*, 2007, **37**, 329-333.
46 R.J. Alkasir, M. Ornatska and S. Andreescu, *Anal. Chem,*. 2012, **84**, 9729-9737.
47 H. K. Maleh, M.Moazampour, A.A. Ensafi, S. Mallakpour and M. Hatami, *Environ Sci Pollut Res*, 2014, **21**, 5879–5888
48 R.L. Sun, Y.Wang, Y.N. Ni and Serge Kokot, *Talanta*, 2014, **125**, 341-346.
49 C. H. Fiske and Y. Subbarow,J. Biol. Chem., 1925, **66**, 375–400.